JACS
JOURNAL OF THE AMERICAN CHEMICAL SOCIETY
Communication
pubs.acs.org/JACS

Reversible On–Off Switching of a Single-Molecule Magnet via a Crystal-to-Crystal Chemical Transformation

Dong-Qing Wu,[†] Dong Shao,[†] Xiao-Qin Wei,[†] Fu-Xing Shen,[†] Le Shi,[†] David Kempe,[‡] Yuan-Zhu Zhang,*[,§] Kim R. Dunbar,*[,‡] and Xin-Yi Wang*[,†]

[†]State Key Laboratory of Coordination Chemistry, Collaborative Innovation Center of Advanced Microstructures, School of Chemistry and Chemical Engineering, Nanjing University, Nanjing 210023, China

[‡]Department of Chemistry, Texas A&M University, College Station, Texas 77840, United States

[§]Department of Chemistry, South University of Science and Technology of China, Shenzhen 518055, China

Supporting Information

ABSTRACT: Dynamic molecular crystals are of high interest due to their potential applications. Herein we report the reversible on–off switching of single-molecule magnet (SMM) behavior in a $[Mo(CN)_7]^{4-}$ based molecular compound. Upon dehydration and rehydration, the trinuclear Mn_2Mo molecule $[Mn(L)(H_2O)]_2[Mo(CN)_7]\cdot 2H_2O$ (**1**) undergoes reversible crystal-to-crystal transformation to a hexanuclear Mn_4Mo_2 compound $[Mn(L)(H_2O)]_2[Mn(L)]_2[Mo(CN)_7]_2$ (**2**). This structural transformation involves the breaking and reforming of coordination bonds which leads to significant changes in the color and magnetic properties. Compound **1** is an SMM with an energy barrier of 44.9 cm^{-1}, whereas **2** behaves as a simple paramagnet despite its higher ground state spin value. The distortion of the pentagonal bipyramidal geometry of $[Mo(CN)_7]^{4-}$ in **2** disrupts the anisotropic exchange interactions that lead to SMM behavior in **1**.

Switchable crystalline materials with tunable physical properties have recently attracted considerable attention owing to their promising applications in molecular devices such as switches and sensors.[1] Materials that undergo single-crystal-to-single-crystal (SCSC) transformations are of particular interest, as they provide excellent platforms for the precise study of structure–property relationship. Understanding these relationships will assist in the design of new switchable materials triggered by events such as guest molecule modification, ligand or metal ion exchange, solid state phase transitions and so on.[1,2] Typically, SCSC transformations are accompanied by the breaking and forming of chemical bonds, which alters the local environment of the metal centers and can even affect the dimensionality of the materials.[3] In molecular magnetic materials, this change can directly modify the magnetic properties including the coupling constant, magnetic anisotropy, magnetic ordering, spin-crossover behavior and slow magnetic relaxation.[3e,f,4,5] The complete on–off switching of single-molecule magnet (SMM) behavior via a SCSC event, however, is very rare.[5c,d]

Another pertinent issue with respect to this work is the fact that SMMs have been studied extensively due to their potential applications in high density information storage, quantum computation, and spintronics.[6−8] In this vein, recent studies initiated in the Dunbar laboratories have focused on the $[Mo^{III}(CN)_7]^{4-}$ anion, which is of particular interest for the potential realization of high T_B SMMs as theoretically predicted in 2003[9] and experimentally confirmed with the Mn_2Mo SMM reported by us in 2013.[10] In contrast to most SMMs whose magnetic anisotropy is based on single-ion contributions,[11a,b] the origin of magnetic anisotropy in the $[Mo^{III}(CN)_7]^{4-}$ based SMM is anisotropic exchange,[11c] which is dependent on the local geometry of $[Mo^{III}(CN)_7]^{4-}$ and the bridging modes of $[Mo^{III}(CN)_7]^{4-}$ to the Mn^{II} ions.[9,10] The SMM behavior can only be observed when the Mo^{III} is bridged to the Mn^{II} ions through the axial CN^- groups; corresponding equatorial isomers are simple paramagnets.[10] Remarkably, although the ground state of the Mn_2Mo compound is only 9/2, the energy barrier reaches 40.5 cm^{-1}. Low dimensional compounds containing $[Mo^{III}(CN)_7]^{4-}$ remain extremely scarce with only several molecular clusters and a few chain compounds having been reported by us.[10,12]

Herein we present details of the reversible SCSC transformation between a trinuclear Mn_2Mo molecule, $[Mn(L)(H_2O)]_2[Mo(CN)_7]\cdot 2H_2O$ (**1**) [L = *N*,*N*′-bis[(1H-imidazol-4-yl)methylene]-2,2-dimethylpropane-1,3-diamine], and a hexanuclear Mn_4Mo_2 compound, $[Mn(L)(H_2O)]_2[Mn(L)]_2[Mo(CN)_7]_2$ (**2**), that occurs upon dehydration and rehydration. The remarkable change in structure involves the cleavage and generation of multiple coordination bonds. Most importantly, this transformation causes subtle geometry changes of $[Mo^{III}(CN)_7]^{4-}$ and alterations in the bridging mode between Mo^{III} and Mn^{II} ions, which, in turn, modifies the magnetic anisotropy and leads to reversible switching of the SMM behavior.

Green single crystals of **1** were prepared by a slow diffusion method under a nitrogen atmosphere (Supporting Information). Although the $[Mo(CN)_7]^{4-}$ anion is extremely air sensitive in solution, the resulting crystals are surprisingly stable in air, even upon heating. Heating green crystals of **1** at 110 °C under a dynamic vacuum for 3 h leads to SCSC conversion to brown crystals of **2**, which return to green upon exposure to

Received: July 6, 2017
Published: August 14, 2017

DOI: 10.1021/jacs.7b07008
J. Am. Chem. Soc. 2017, 139, 11714–11717

moisture for 5 h. The reversible transformation process between **1**↔**2** is fully supported by single crystal and powder X-ray diffraction studies (Figure S1) as well as variable-temperature FTIR and UV−vis spectra (Figures S3, S4). The changes in color (green↔brown) (Figure S2), structure (trinuclear↔hexanuclear), and magnetic response (SMM on↔SMM off) are dramatic, but, remarkably, the structural integrity of the single crystal is maintained.

Compound **1** crystallizes in the monoclinic space group *C*2/*c* and exhibits a trinuclear Mn_2Mo structure. The asymmetric unit contains one-half of a $[Mo(CN)_7]^{4-}$ anion, a $Mn^{II}L$ unit, a coordinated water molecule, and an interstitial water molecule. The $[Mo(CN)_7]^{4-}$ anion is only slightly distorted from the ideal D_{5h} pentagonal bipyramidal (PBP) geometry with a continuous shape measure (CShM) value of only 0.291 (Figure S5, Table S3).[13] The near-perfect PBP geometry is extremely important for the SMM behavior of **1** because Mo^{III} exhibits the greatest potential for Ising-type anisotropic exchange in the axial D_{5h} geometry.[9] The Mn^{II} ion is coordinated to four N atoms from the ligand L, one N atom from a bridging CN^-, and an O atom from the coordinated water, resulting in a distorted trigonal prism (CShM = 1.150). Bridged by two axial CN^- groups, one Mo^{III} and two Mn^{II} ions form the trinuclear Mn_2Mo cluster. The Mo—C—N bond angles in the Mo—C≡N—Mn linkages are close to linear with a value of 179.5(3)°, whereas the C—N—Mn bond angle is 168.0(3)°. These structural features are very similar to the reported Mn_2Mo SMM,[10] and are consistent with its observed SMM behavior (vide infra).

The coordinated water (O1) is hydrogen bonded to a terminal N atom (N3A) of the $[Mo(CN)_7]^{4-}$ from an adjacent Mn_2Mo unit (O1···N3A = 2.782(5) Å) and also to two solvent water molecules (O1···O2 = 2.846(5) and O1···O2A = 2.861(4) Å). Connected by these H-bonds, the Mn_2Mo units form a one-dimensional structure (Figure S6, Table S4), in which the distance between the N3A atom and the Mn1 ion of the adjacent Mn_2Mo unit is only 4.421(3) Å. The N3 atom coordinates to the Mn^{II} ion of the adjacent Mn_2Mo unit after removal of the O1 atom, and is therefore responsible for the SCSC transformation.

After dehydration, the space group of **2** changes to monoclinic *C*2/*m*. The asymmetric unit contains one-half of a $[Mo(CN)_7]^{4-}$ anion, two halves of the $Mn^{II}L$ subunit, and one-half of a coordinated water molecule. It is noted that half of the coordinated water molecule (O1) and all the interstitial water molecules (O2) in **1** can be removed easily, whereas the other half of O1 remains in the structure even after the crystal is heated at 110 °C under vacuum for 10 h or heated on the X-ray diffractometer to 160 °C (Supporting Information). Further attempts to remove all the water molecules while maintaining the integrity of the single crystal failed due to cracking of the crystal upon heating to higher temperatures. In **2**, the coordination geometry of Mo^{III} is best described as a capped trigonal prism (Figure S5, Table S3). The Mn1 ion is in a N_5O_1 environment with an elongated Mn—O bond length of 2.767(13) Å, whereas Mn2 is coordinated to six N atoms. The structure of **2** is a neutral Mn_4Mo_2 hexanuclear cluster (Figure 1). Each $[Mo(CN)_7]^{4-}$ unit links three $Mn^{II}L$ units via three cyanide bridges. Two of them (C1N1 and C5N5) are originally in the axial position in **1** and the new bridging cyanide (C3N3) is in the original equatorial position of **1**. The Mo—C—N bond angles in the Mo—C≡N—Mn linkages are all close to linear with values of 176.1(5)°, 176.9(5)°, and 174.3(5)°, whereas the related C—N—Mn bond angles are slightly bent, being 159.5(5)°, 169.3(5)°, 172.5(4)°, respectively. The hexanuclear molecules are further organized by weak hydrogen bonds (Figure S8, Table S4).

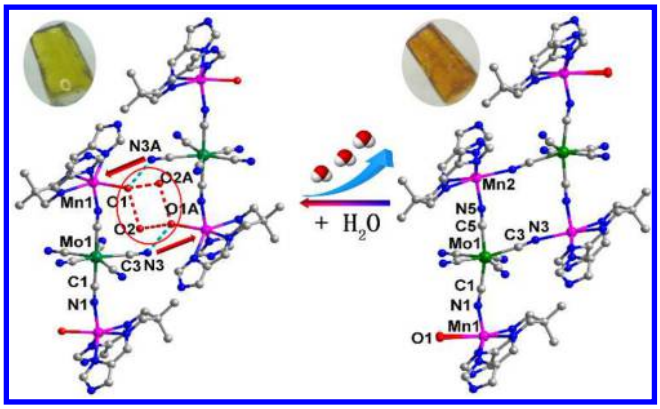

Figure 1. Structures of the trinuclear Mn_2Mo and hexanuclear Mn_4Mo_2 clusters in **1** and **2**. The water molecules in the red circle were removed by dehydration and the red arrows indicate the formation of the new Mn—N bonds.

Variable temperature magnetic susceptibilities of **1** were collected at a 1 kOe dc field (Figure 2). Upon cooling, the $\chi_M T$ value for each $Mn^{II}_2Mo^{III}$ decreases from 9.01 $cm^3\ mol^{-1}K$ at 300 K to a minimum of 8.51 $cm^3\ mol^{-1}K$ at 90 K, increases to a maximum of 14.14 $cm^3\ mol^{-1}K$ at 4 K, and finally decreases to 9.57 $cm^3\ mol^{-1}K$ at 2 K. The decrease in $\chi_M T$ above 80 K suggests a dominant AF interaction. It has been reported for the previous trinuclear Mn_2Mo compound with two axial CN^- bridges,[10,14] that an Ising-type anisotropic exchange interaction ($J_z = -17$, $J_{xy} = -5.5$ cm^{-1} with $H_{eff} = -2J_{xy}(S^x_{Mo}S^x_{Mn} + S^y_{Mo}S^y_{Mn}) - 2J_zS^z_{Mo}S^z_{Mn}$) is responsible for its magnetic anisotropy and SMM behavior. A similar approach was used to fit the magnetic susceptibility of **1** above 6 K using PHI,[15] leading to a very similar Ising type anisotropic coupling interaction of $J_z = -17.7$, $J_{xy} = -5.7$ cm^{-1} (Figure 2).

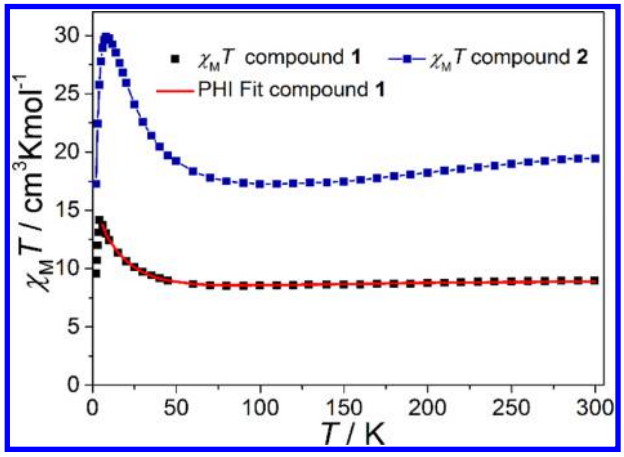

Figure 2. Temperature dependence of $\chi_M T$ for **1** and **2**. The red line is the best fit using the model described in the text.

The dynamic magnetic properties of **1** were also investigated (Figure 3, S10 and S11). A pronounced frequency dependence was observed with a shift parameter $\varphi = (\Delta T_p/T_p)/\Delta(\log f) = 0.14$, which is in the normal range for an SMM. Furthermore, hysteresis loops were observed from 1.8 to 3.0 K at different field sweep rates (Figure S12, S13), which confirms the SMM

DOI: 10.1021/jacs.7b07008
J. Am. Chem. Soc. 2017, 139, 11714−11717

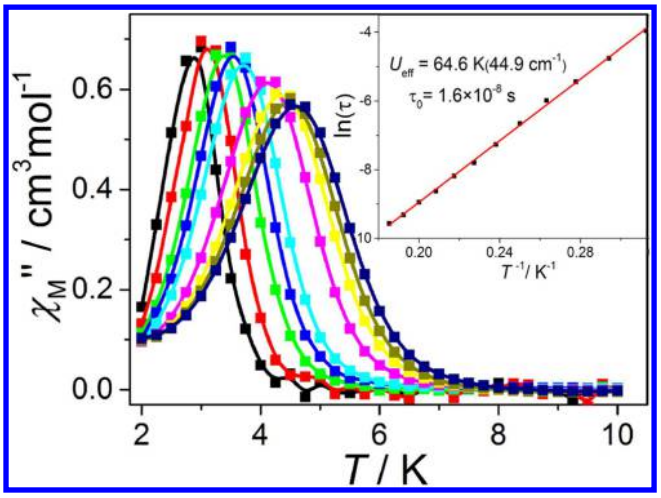

Figure 3. Temperature dependent out-of-phase χ_M'' for **1** under H_{ac} = 2 Oe and H_{dc} = 0 Oe; the Arrhenius plot of **1** (inset).

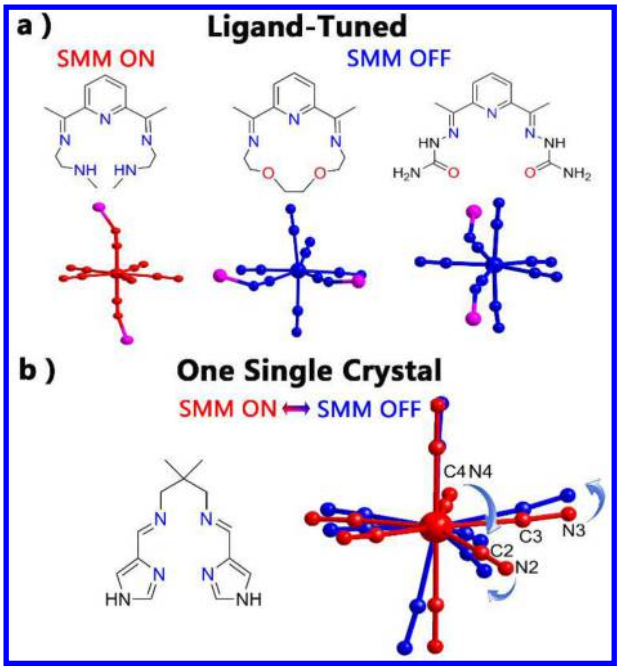

Figure 4. Summary of different strategies to tune the SMM behavior of the Mn–Mo clusters based on $[Mo(CN)_7]^{4-}$. The SMM behavior can be switched on and off by (a) using different ligands to tune the final structures and (b) through the SCSC transformation of one single crystal. The red and blue colors in panel b represent the $[Mo(CN)_7]^{4-}$ units before and after dehydration, and the arrows indicate the movements of the cyanide groups.

behavior of **1**. The Cole–Cole plots at 3.2 to 5.4 K of **1** can be fitted well with the generalized Debye model (Figure S14). The α parameters are in the range of 0.15 to 0.35 (Table S5), suggesting a narrow distribution of relaxation times.[16] From the fit of the relaxation time τ to $1/T$ according to the Arrhenius law $\tau = \tau_0 \exp(U_{eff}/k_B T)$ (Figure 3c), the effective energy barrier (U_{eff}) was estimated to be U_{eff} = 44.9 cm^{-1} (64.6 K) with τ_0 = 1.6 × 10^{-8} s (R^2 = 0.999). This energy barrier is slightly higher than that of 40.5 cm^{-1} (58.5 K) for the reported Mn_2Mo SMM,[10] which makes it the new record for cyanide-based SMMs.

For **2**, the decrease in $\chi_M T$ above 100 K along with isothermal magnetization data measured at 2 K (Figure S15) indicate a dominant AF interaction. Details of the Mo^{III}—Mn^{II} magnetic coupling, however, cannot be extracted even if all these interactions are considered isotropic, as there are at least three different magnetic interaction pathways (through the C1N1, C3N3, and C5N5 linkages). Considering the higher ground spin state of **2**, it would be reasonable to anticipate that **2** may be a better SMM than **1**. However, ac susceptibilities of **2** measured at zero dc field did not exhibit any χ_M'' signals (Figure S16), ruling out its SMM behavior.

A careful analysis of the structures reveals that the lack of SMM behavior is related to the different coordination geometry of Mo^{III} in these structures. In our previous studies,[10] we established that the SMM behavior of the linear trinuclear Mn_2Mo compound could be quenched by using different organic ligands that led to equatorial rather than axial isomers; the former molecules behave as simple paramagnets (Figure 4a).[10] Theoretical studies by Mironov revealed that this difference is due to the anisotropic exchange being Ising-type for the axial bridged Mn–NC–Mo linkages and easy-plane for the equatorial analogues. For the hypothetical Mn_4Mo_2 compound,[14] the Mo^{III} centers are still in a PBP geometry, but a comparison of the structures of **1** and **2** reveals that, during dehydration, whereas the two axial cyano groups remain connected to the Mn^{II} centers, the C3N3 group in **1** tilts away from the equatorial plane toward the vacant coordination site (after removal of the coordination water O1) of the Mn^{II} center in the adjacent Mn2Mo unit. At the same time, the other two cyanide groups (C2N2 and C4N4) bend away from the equatorial plane (Figure 1, Figure 4b). Consequently, the coordination geometry of the Mo^{III} center distorts significantly from the pentagonal bipyramid to the capped trigonal prism as evidenced by the CShM values (Figure S3 and Table S3). This significant distortion from axial D_{5h} geometry greatly reduces the orbital contribution and also the spin–orbit coupling of the Mo^{III} center which compromises the origin of the anisotropic exchange and switches off the SMM behavior in **2**. Finally, it is important to point out that ideal pentagonal bipyramidal D_{5h} symmetry has recently been found to have important implications for lanthanide based SMMs as well, leading to very high U_{eff} and T_B values for Dy^{III} SMMs and novel magnetic properties for a Ho^{III} complex.[17]

In summary, we have discovered reversible on and off switching of SMM behavior achieved by SCSC transformation between trinuclear Mn_2Mo and hexanuclear Mn_4Mo_2 molecules based on the heptacyanomolybdate(III) anion. The transformation involves cleavage and generation of multiple coordination bonds, the result of which are changes in the coordination geometry of the Mo^{III} center, the bridging mode of the CN groups, the nuclearity of the molecules as well as the magnetic coupling interactions between the spin centers and their magnetic properties. These results highlight the importance of the SCSC transformation in the study of dynamic molecular systems and underscore the importance of anisotropic magnetic coupling for the elaboration of high T_B SMM in our pursuit of molecular magnetic materials of heptacyanomolybdate(III).

■ ASSOCIATED CONTENT

Supporting Information

The Supporting Information is available free of charge on the ACS Publications website at DOI: 10.1021/jacs.7b07008.

DOI: 10.1021/jacs.7b07008
J. Am. Chem. Soc. 2017, 139, 11714–11717

Experimental details, crystallographic data, additional figures and tables (PDF)
X-ray crystallographic files (CIF)

AUTHOR INFORMATION

Corresponding Authors

*wangxy66@nju.edu.cn
*dunbar@mail.chem.tamu.edu
*zhangyz@sustc.edu.cn

ORCID

Dong Shao: 0000-0002-3253-2680
Kim R. Dunbar: 0000-0001-5728-7805
Xin-Yi Wang: 0000-0002-9256-1862

Notes

The authors declare no competing financial interest.

ACKNOWLEDGMENTS

K.R.D. acknowledges funding from the U.S. Department of Energy, Basic Energy Sciences, Materials Sciences Division under Grant DE-SC0012582. K.R.D. is also grateful to the Robert A. Welch Foundation for financial support (A-1449). X.-Y.W. thanks the Major State Basic Research Development Program (2013CB922102), NSFC (21522103, 21471077, 91622110) and the NSF of Jiangsu province (BK20150017).

REFERENCES

(1) (a) *Handbook of Stimuli-Responsive Materials*; Urban, M. W., Ed.; Wiley-VCH: Weinheim, 2011. (b) Naumov, P.; Chizhik, S.; Panda, M. K.; Nath, N. K.; Boldyreva, E. *Chem. Rev.* **2015**, *115*, 12440−12490. (c) Sato, O. *Nat. Chem.* **2016**, *8*, 644−656.

(2) (a) Kole, G. K.; Vittal, J. J. *Chem. Soc. Rev.* **2013**, *42*, 1755−1775. (b) Wang, H.-R.; Meng, W.; Wu, J.; Ding, J.; Hou, H.-W.; Fan, Y.-T. *Coord. Chem. Rev.* **2016**, *307*, 130−146.

(3) (a) Hu, C. H.; Englert, U. *Angew. Chem., Int. Ed.* **2005**, *44*, 2281−2283. (b) Ghosh, S. K.; Kaneko, W.; Kiriya, D.; Ohba, M.; Kitagawa, S. *Angew. Chem., Int. Ed.* **2008**, *47*, 8843−8847. (c) Medishetty, R.; Koh, L. L.; Kole, G. K.; Vittal, J. J. *Angew. Chem., Int. Ed.* **2011**, *50*, 10949−10952. (d) Zhang, Z.-X.; Ding, N.-N.; Zhang, W.-H.; Chen, J.-X.; Young, D. J.; Hor, T. S. A. *Angew. Chem., Int. Ed.* **2014**, *53*, 4628−4632. (e) Rodríguez-Jiménez, S.; Feltham, H. L. C.; Brooker, S. *Angew. Chem., Int. Ed.* **2016**, *55*, 15067−15071. (f) Zhang, Y.-J.; Liu, T.; Kanegawa, S.; Sato, O. *J. Am. Chem. Soc.* **2009**, *131*, 7942−7943.

(4) (a) Nihei, M.; Han, L.-Q.; Oshio, H. *J. Am. Chem. Soc.* **2007**, *129*, 5312−5313. (b) Neville, S. M.; Halder, G. J.; Chapman, K. W.; Duriska, M. B.; Southon, P. D.; Cashion, J. D.; Létard, J. F.; Moubaraki, B.; Murray, K. S.; Kepert, C. J. *J. Am. Chem. Soc.* **2008**, *130*, 2869−2876. (c) Wriedt, M.; Yakovenko, A. A.; Halder, G. J.; Prosvirin, A. V.; Dunbar, K. R.; Zhou, H.-C. *J. Am. Chem. Soc.* **2013**, *135*, 4040−4050. (d) Costa, J. S.; Rodríguez-Jiménez, S.; Craig, G. A.; Barth, B.; Beavers, C. M.; Teat, S. J.; Aromí, G. *J. Am. Chem. Soc.* **2014**, *136*, 3869−3874. (e) Murphy, M. J.; Zenere, K. A.; Ragon, F.; Southon, P. D.; Kepert, C. J.; Neville, S. M. *J. Am. Chem. Soc.* **2017**, *139*, 1330−1335.

(5) (a) Zhang, X.-J.; Vieru, V.; Feng, X.-W.; Liu, J.-L.; Zhang, Z. − J; Na, B.; Shi, W.; Wang, B.-W.; Powell, A. K.; Chibotaru, L. F.; Gao, S.; Cheng, P.; Long, J. R. *Angew. Chem., Int. Ed.* **2015**, *54*, 9861−9865. (b) Liu, J.-L.; Chen, Y.-C.; Zheng, Y.-Z.; Lin, W.-Q.; Ungur, L.; Wernsdorfer, W.; Chibotaru, L. F.; Tong, M.-L. *Chem. Sci.* **2013**, *4*, 3310−3316. (c) Vallejo, J.; Pardo, E.; Viciano-Chumillas, M.; Castro, I.; Amorós, P.; Déniz, M.; Ruiz-Pérez, C.; Yuste-Vivas, C.; Krzystek, J.; Julve, M.; Lloret, F.; Cano, J. *Chem. Sci.* **2017**, *8*, 3694−3702. (d) Zhou, Q.; Yang, F.; Xin, B. -J; Zeng, G.; Zhou, X. J.; Liu, K.; Ma, D. X.; Li, G. − M.; Shi, Zh.; Feng, S.-H. *Chem. Commun.* **2013**, *49*, 8244−8246.

(6) Vincent, R.; Klyatskaya, S.; Ruben, M.; Wernsdorfer, W.; Balestro, F. *Nature* **2012**, *488*, 357−360.

(7) (a) Bogani, L.; Wernsdorfer, W. *Nat. Mater.* **2008**, *7*, 179−186. (b) Cervetti, C.; Rettori, A.; Pini, M. G.; Cornia, A.; Repolles, A.; Luis, F.; Dressel, M.; Rauschenbach, S.; Kern, K.; Burghard, M.; Bogani, L. *Nat. Mater.* **2016**, *15*, 164−168.

(8) (a) Leuenberger, M. N.; Loss, D. *Nature* **2001**, *410*, 789−793. (b) Schlegel, C.; van Slageren, J.; Manoli, M.; Brechin, E. K.; Dressel, M. *Phys. Rev. Lett.* **2008**, *101*, 147203.

(9) Mironov, V. S.; Chibotaru, L. F.; Ceulemans, A. *J. Am. Chem. Soc.* **2003**, *125*, 9750−9760.

(10) Qian, K.; Huang, X.-C.; Zhou, C.; You, X.-Z.; Wang, X.-Y.; Dunbar, K. R. *J. Am. Chem. Soc.* **2013**, *135*, 13302−13305.

(11) (a) Woodruff, D. N.; Winpenny, R. E. P.; Layfield, R. A. *Chem. Rev.* **2013**, *113*, 5110−5148. (b) Bar, A. K.; Pichon, C.; Sutter, J. P. *Coord. Chem. Rev.* **2016**, *308*, 346−380. (c) Palii, A.; Tsukerblat, B.; Clemente-Juan, J. M.; Coronado, E. *Int. Rev. Phys. Chem.* **2010**, *29*, 135−230.

(12) (a) Wang, X.-Y.; Prosvirin, A. V.; Dunbar, K. R. *Angew. Chem., Int. Ed.* **2010**, *49*, 5081−5084. (b) Wei, X.-Q.; Qian, K.; Wei, H.-Y.; Wang, X.-Y. *Inorg. Chem.* **2016**, *55*, 5107−5109. (c) Wang, K.; Xia, B.; Wang, Q.-L.; Ma, Y.; Liao, D. − Z.; Tang, J.-K. *Dalton Trans.* **2017**, *46*, 1042−1046.

(13) Llunell, M.; Casanova, D.; Cirera, J.; Alemany, P.; Alvarez, S. *SHAPE*, Version 2.1; Universitat de Barcelona: Barcelona, 2013.

(14) Mironov, V. S. *Inorg. Chem.* **2015**, *54*, 11339−11355.

(15) Chilton, N. F.; Anderson, R. P.; Turner, L. D.; Soncini, A.; Murray, K. S. *J. Comput. Chem.* **2013**, *34*, 1164−1175.

(16) Cole, K. S.; Cole, R. H. *J. Chem. Phys.* **1941**, *9*, 341−352.

(17) (a) Ding, Y.-S.; Chilton, N. F.; Winpenny, R. E. P.; Zheng, Y.-Z. *Angew. Chem., Int. Ed.* **2016**, *55*, 16071−16074. (b) Chen, Y.-C.; Liu, J.-L.; Ungur, L.; Liu, J.; Li, Q.-W.; Wang, L.-F.; Ni, Z.-P.; Chibotaru, L. F.; Chen, X.-M.; Tong, M.-L. *J. Am. Chem. Soc.* **2016**, *138*, 2829−2837. (c) Chen, Y.-C.; Liu, J.-L.; Wernsdorfer, W.; Liu, D.; Chibotaru, L. F.; Chen, X.-M.; Tong, M.-L. *Angew. Chem.* **2017**, *129*, 5078−5082.

DOI: 10.1021/jacs.7b07008
J. Am. Chem. Soc. 2017, 139, 11714−11717